Available online at www.sciencedirect.com
SCIENCE DIRECT®
Journal of Power Sources 132 (2004) 275–281
JOURNAL OF POWER SOURCES
www.elsevier.com/locate/jpowsour

Studies of pasted nickel electrodes to improve cylindrical nickel–zinc cells

Waltraud Taucher-Mautner*, Karl Kordesch

Institute for Chemical Technology of Inorganic Materials, Graz University of Technology, Stremayrgasse 16, A-8010 Graz, Austria

Received 25 November 2003; accepted 6 January 2004

Abstract

The aim of the present paper was to study the influence of foam type as well as nickel and cobalt additives on cell performance and cycle life of cylindrical nickel–zinc cells. Experiments have shown that discharge capacity depends on the foam type of nickel electrodes and is significantly improved by using thicker foam substrates (2.2 mm). AA-size nickel–zinc cells constructed of two thinner nickel electrode layers (1.6 mm) displayed stronger decline in capacity during cycle life due to a very low zinc/nickel hydroxide ratio (1.1–1.2). The addition of nickel and cobalt powder was investigated by means of resistivity measurements of PVA-bonded nickel hydroxide films. This study elucidated that small amounts of cobalt (2–8 wt.%) caused an extreme decline in resistivity. Admixture of nickel also lowered resistivity but not as great as cobalt. The cell performance turned out to be contrary to resistivity measurements; nickel–zinc cells prepared with a less conductive slurry delivered higher capacities. However, discharge capacity decreased rapidly after prolonged cell cycling, as the zinc/nickel hydroxide ratio of these cells was also considerably reduced.

Keywords: Nickel–zinc cells; Cylindrical design; Pasted nickel electrodes; Foam thickness; Cobalt and nickel additives; Cycle life

1. Introduction

Rechargeable nickel–zinc cells represent a very attractive power supply with the advantage of reduced environmental impact compared to the Ni–Cd system and are much less expensive than Ni–MH cells. The nickel–zinc cell delivers very high specific energy (55–85 Wh/kg) and high specific power (140–200 W/kg) and the nominal cell voltage of 1.6 V is 400 mV higher than for Ni–Cd and Ni/MH cells. Although research on nickel–zinc cells of flat plate design has been done for many years [1–12], less effort has been made to build a cylindrical nickel–zinc cell [13–15]. The development and progress of nickel–zinc cells until 1998 was extensively reviewed by Jindra [16–18] and well documented by other authors [19–21]. Recently, the cycle life limitation of nickel–zinc cells associated with the solubility of the zinc electrode was overcome by Bugnet et al. [22,23] through stabilising the zinc electrode with a three dimensional current collector network, conductive ceramics and anti-polar additives.

The electrochemical reaction (discharge/charge) of nickel–zinc cells can be formulated as:

$$2\,\mathrm{NiOOH} + \mathrm{Zn} + 2\,\mathrm{H_2O} \rightleftharpoons 2\,\mathrm{Ni(OH)_2} + \mathrm{Zn(OH)_2}. \quad (1)$$

In addition to this current-generating process, two parasitic side reactions occur during overcharge: (i) oxygen formation at the nickel electrode, and (ii) hydrogen evolution at the zinc electrode:

$$4\,\mathrm{OH^-} \rightleftharpoons 2\,\mathrm{H_2O} + \mathrm{O_2} + 4\,\mathrm{e^-} \quad (2)$$

$$2\,\mathrm{H_2O} + 2\,\mathrm{e^-} \rightleftharpoons \mathrm{H_2} + 2\,\mathrm{OH^-}. \quad (3)$$

Nickel–zinc cells have to be slightly overcharged to receive better charge acceptance of the nickel electrode, however, at the end of charging, oxygen gas builds up at the nickel electrode. But in the case of good access to the zinc electrode, oxygen can be directly recombined at metallic zinc particles [16,24]. In order to minimise parasitic hydrogen evolution at the zinc electrode during overcharging, nickel–zinc cells have to be balanced in a nickel-limited way (Zn/Ni ratio > 1). The recombination of hydrogen at the nickel electrode is accelerated by small amounts of silver oxide catalyst.

In this study we have continued previous work on cylindrical nickel–zinc cells that were made of sintered nickel electrodes dismantled from commercial Ni–Cd cells [25].

* Corresponding author. Tel.: +43-316-873-8269; fax: +43-316-873-8272.
E-mail address: waltraud.taucher-mautner@tugraz.at (W. Taucher-Mautner).

0378-7753/$ – see front matter © 2004 Elsevier B.V. All rights reserved.
doi:10.1016/j.jpowsour.2004.01.032

Furthermore, a pasting procedure was developed and different binder materials (PVA, Teflon) were investigated to prepare lightweight nickel electrodes [26,27]. Pasted nickel electrodes deliver enormous weight saving in cathode mass up to 50% compared to sintered nickel electrodes. The main objective of the present paper is focused on the nickel electrode, especially on foam type and composition of nickel hydroxide slurry, to improve cell capacity and cycle life of cylindrical nickel–zinc cells.

2. Experimental

2.1. Preparation of nickel hydroxide electrode

Nickel hydroxide electrodes used as cathodes for cylindrical nickel–zinc cells were fabricated in our laboratory. A 2–8.6 wt.% nickel powder (Type 210, Inco), 2–8 wt.% extra-fine cobalt powder (Carolmet Cobalt Products, Union Miniere, Inc.) and 0.2 wt.% silver(I)-oxide (Aldrich) was blended and after that mixed with 30 wt.% polyvinylalcohol (PVA) solution (1.2 wt.% PVA solution, Fluka) as a binder. Finally, 53.2–65.8 wt.% spherical nickel hydroxide (Inco) and a small amount of water was added to obtain a light nickel hydroxide suspension that can easily penetrate into the nickel foam. This nickel hydroxide slurry was pasted on both sides of the nickel foam coupon several times to ensure homogeneous distribution of nickel hydroxide particles throughout the nickel foam. After the pasting procedure wet electrodes were dried at 110 °C for 1 h.

2.2. Preparation of zinc electrode

The preparation of zinc electrode was carried out by mixing of the dry components: 59 wt.% zinc oxide (Merck), 10 wt.% zinc (Type 004F, Union Miniere SA) and 0.5 wt.% gelling agent (Carbopol, Type 940, Nacan) and adding 30.5 wt.% of a 7 M potassium hydroxide solution (Merck) as the electrolyte. The addition of zinc powder to the main component zinc oxide improved electronic conductivity of the gelatinous zinc electrode.

2.3. Production of cylindrical nickel–zinc cell

Fig. 1 summarises the single steps of cylindrical nickel–zinc cell production on a laboratory scale. First, the nickel foam was cut into the specified size, and a nickel foil current collector was spotwelded along the lower edge of the foam. Next, the nickel hydroxide slurry was prepared and pasted into the nickel foam as described previously. A separator bag, consisting of two layers of a laminate of high-purity cellulose film bonded to a non-woven polyamide fibre (Berec Components Ltd.), was formed and the dry nickel electrode was rolled up around it. This assembled unit was then inserted into the nickel-plated steel can and overnight electrolyte soaking (27 wt.% KOH, 10 g/l LiOH × H_2O) followed. Finally, the half-finished cell was filled with zinc anode gel and closed.

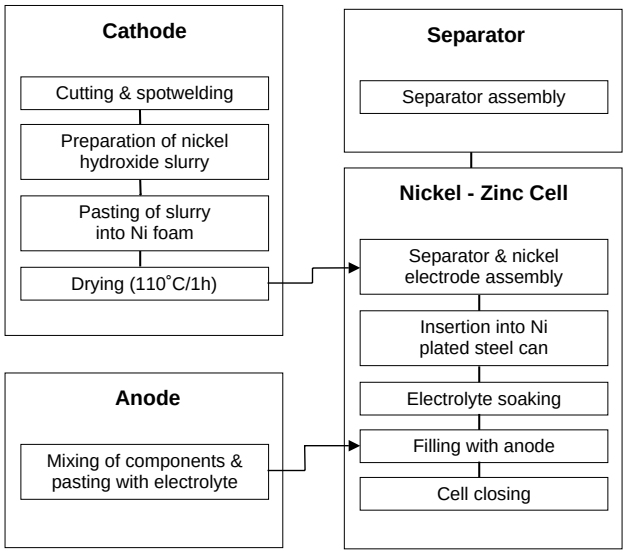

Fig. 1. Cylindrical nickel–zinc cell laboratory production.

In Fig. 2 the cross-section of a cylindrical nickel–zinc cell is shown. Nickel hydroxide cathode and zinc anode were prepared in our laboratory according to the above procedures. The nickel-plated steel can and the cell closure were commercial products used in primary and rechargeable alkaline manganese dioxide zinc (RAM^{TM}) cells [28].

2.4. Cell testing

The cycling programme of cylindrical nickel–zinc cells can be seen in Fig. 3. The cells were tested with

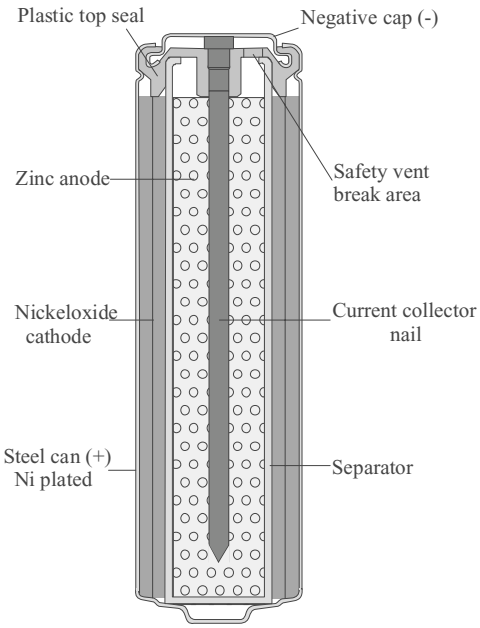

Fig. 2. Cross-section of a cylindrical nickel–zinc cell.

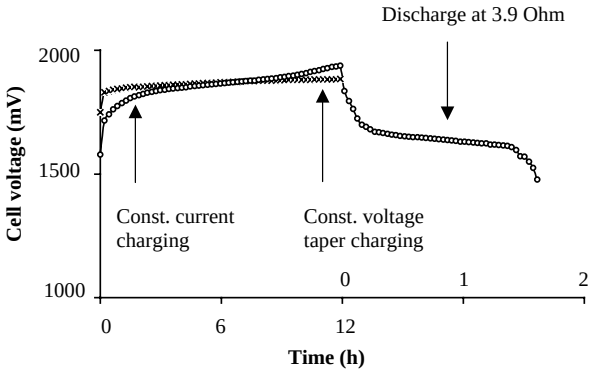

Fig. 3. Cycling programme of AA-size nickel–zinc cells. Charge: constant voltage taper charging (1.90 V, approximately 8 h) or constant current charging (50–100 mA, 6–12 h). Discharge: at 3.9 Ω–800 mV.

a computer-controlled multi-channel testing system that runs the following cycling regime: cells were either charged with constant voltage (1.90 V) or with constant current (50–100 mA) for 6–12 h. Discharge cycles were performed at 3.9 Ω to a cut-off voltage of 800 mV.

Constant current charging demands precise charging time adjustment or voltage limitation (1.90–1.95 V) to prevent extended overcharging. Otherwise, large quantities of oxygen would be generated that might cause pressure increase and cell leakage. In the case of constant voltage taper charging, the initial current can be as high as 500 mA. However, at the end of the charging process a low residual current of 10–20 mA flows and switching off is not very critical in this mode. Therefore, the charging of cells in this study was carried out with constant voltage at 1.90 V.

3. Results and discussion

3.1. Morphological characterisation

The morphology of nickel foam and pasted nickel electrode was examined by means of scanning electron microscopy (SEM). In Fig. 4 SEM pictures of nickel foam (a) and pasted nickel electrode (b) are shown. Image 1a presents the high-porous structure of a 2.2 mm thick nickel foam containing pores of approximately 100–200 μm. In picture 1b the surface of the pasted nickel electrode can be seen. The spherical particles of various diameters range from 1 up to 10 μm and depict nickel hydroxide. The non-spherical particles are metallic nickel and cobalt powders with a particle size of 1 μm and below. It can be seen that nickel hydroxide spheres are homogeneously distributed on the nickel foam. Small nickel and cobalt particles are embedded between the larger nickel hydroxide spheres to provide sufficient electronic conductivity of the electrode.

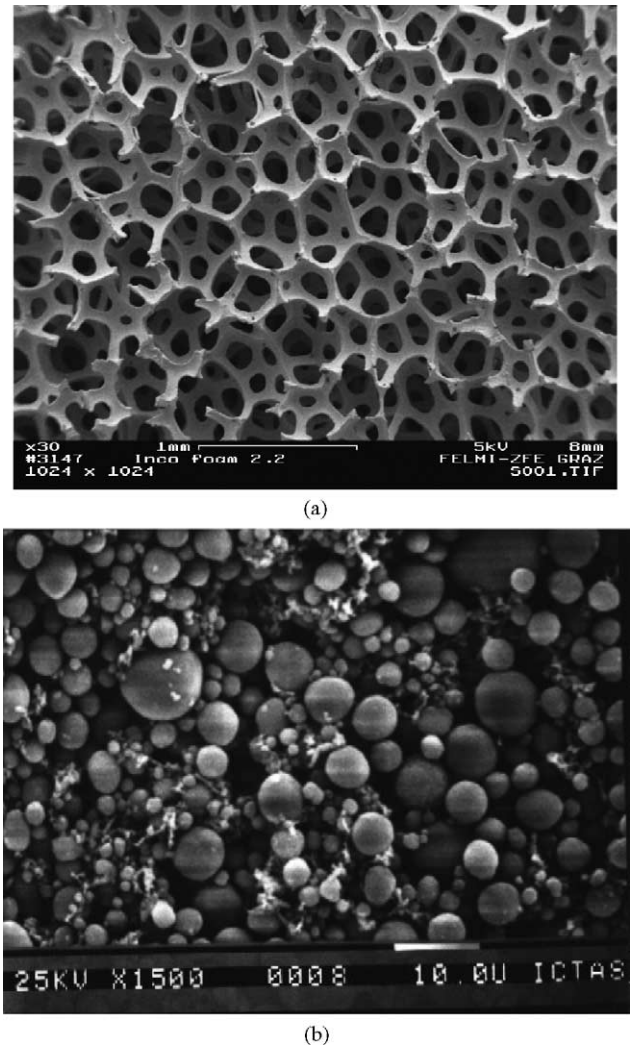

Fig. 4. SEM images of (a) nickel foam (Inco, 2.2 mm); (b) nickel electrode prepared by pasting of nickel foam with nickel hydroxide slurry of composition A.

3.2. Cell performance of nickel–zinc cells with one or two nickel hydroxide layers

Nickel foam is commercially available in a variety of thickness and porosity. This study focused on the investigation of pasted nickel electrodes with foam thicknesses of 1.6, 1.9 and 2.2 mm and a porosity of 80 and 110 pores per inch (PPI) for application in AA-size nickel–zinc cells as listed in Table 1. Due to the fact that the cylindrical cell de-

Table 1
Types of nickel foam used for pasted nickel hydroxide electrodes of AA-size Ni–Zn cells

Nickel foam type[a]	Thickness (mm)	1 and 2 layers (mm × mm)
Retec 80 PPI	1.6	38 × 36/70
Retec 110 PPI	1.6	38 × 36/70
Inco	1.9	38 × 36
Inco	2.2	38 × 36

[a] Supplier: Retec foam, RPM Ventures, ELTEC Systems Corp.; Ohio Inco foam, Inco Technical Services Ltd., Mississauga, Ontario.

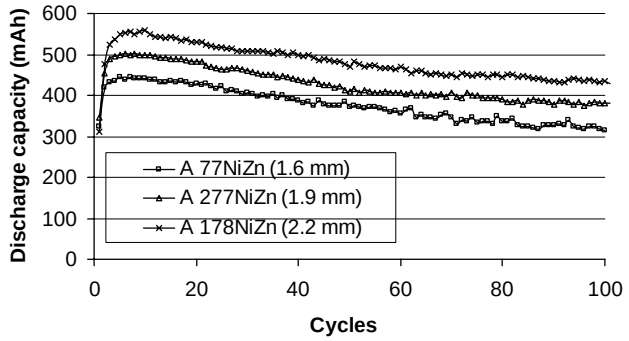

Fig. 5. Discharge capacity of AA-size nickel–zinc cells with one layer of nickel hydroxide electrode of different foam thickness vs. cycles. Discharge: at 3.9 Ω–800 mV. Charge: with 1.90 V constant.

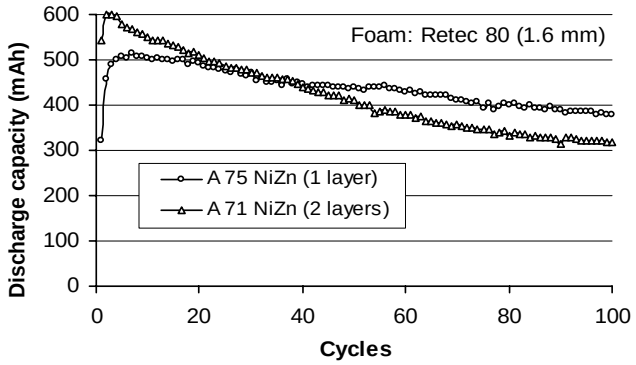

Fig. 6. Discharge capacity of AA-size nickel–zinc cells with one nickel layer and two nickel layers vs. cycles. Discharge: at 3.9 Ω–800 mV. Charge: with 1.90 V constant.

sign is volume limited, AA-size nickel–zinc cells could only be prepared with one or two nickel layers according to the applied foam thickness. The single-layered nickel electrode arrangement was carried out for all foam samples. Cylindrical nickel–zinc cells comprising the 1.6 mm foam type were also constructed in a double-layered version.

Fig. 5 shows the discharge capacity of AA-size nickel–zinc cells built of one layer of nickel hydroxide electrode of different foam thickness versus cycles. These curves exhibit a relatively flat discharge profile with only small capacity decline up to 100 cycles. The first few cycles represent formation cycles; discharge capacity is initially low but increases quickly during the next cycles to reach its maximum after 5–10 cycles. This figure clearly demonstrates that discharge capacity depends on foam thickness. The thicker foam material offers the advantage of pasting a higher amount of nickel hydroxide slurry into the foam substrate of these cells, as presented in Table 2, and thus to increase discharge capacity. The best result is yielded with the 2.2 mm foam. Discharge capacity was enormously improved by 25% (10th cycle) to 34% (100th cycle) compared to a 1.6 mm foam.

Figs. 6 and 7 compare nickel–zinc cells constructed with one nickel hydroxide layer to cells prepared with two layers of the 1.6 mm foam type (Retec 80 and 110). Cylindrical nickel–zinc cells containing double-layered nickel hydroxide electrodes delivered very high capacities of 600–500 mAh during the first 20 cycles. Between the 20th and the 50th cycle, discharge capacity nearly equalled the performance of cells with single-layered electrodes; beyond that, capacity was considerably lower. Both figures clearly display that nickel–zinc cells made of two nickel hydroxide layers show much stronger decline in capacity during cycle life. In our study we observed that this behaviour correlated

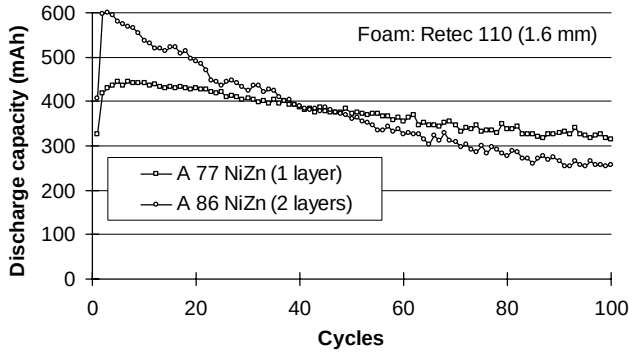

Fig. 7. Discharge capacity of AA-size nickel–zinc cells with one nickel layer and two nickel layers vs. cycles. Discharge: at 3.9 Ω–800 mV. Charge: with 1.90 V constant.

Table 2
AA-size Ni–Zn cells containing various nickel electrodes with one or two nickel layers

Cell number[a]	No. of layers[b]	Zn-anode (g)	Ni-cathode (g)	Zn/Ni(OH)$_2$ ratio	Ni(OH)$_2$ utilisation (%)[c]
A 71 (A)	2 (R1)	3.00	4.14	1.19	59.7
A 75 (A)	1 (R1)	6.00	2.83	2.62	76.4
A 86 (A)	2 (R2)	3.00	4.41	1.12	54.1
A 77 (A)	1 (R2)	6.00	2.31	3.21	81.7
A 277 (B)	1 (I1)	4.00	2.95	2.40	72.9
A 178 (B)	1 (I2)	4.00	3.71	1.78	64.3
A 145 (C)	1 (I2)	4.00	4.26	1.39	56.6

Cells were discharged at 3.9 Ω–800 mV and charged at 1.90 V constant.
[a] Nickel hydroxide slurry composition: (A) 4.29% Co, 8.57% Ni; (B) 8% Co, 8.57% Ni; (C) 4.29% Co, 2% Ni.
[b] Foam type: (R1) Retec 80/1.6 mm; (R2) Retec 110/1.6 mm; (I1) Inco/1.9 mm; (I2) Inco/2.2 mm.
[c] Calculation based on the fifth discharge cycle.

to the zinc/nickel hydroxide ratio. The double-layered electrode type has less space available for the zinc electrode, and therefore a very low zinc/nickel hydroxide ratio was obtained in these cells. No great difference in cycling behaviour was observed between cells with Retec 80 and 110 foam. Cell A 77NiZn delivered a slightly lower discharge capacity curve as less nickel hydroxide slurry was pasted into the foam.

Table 2 summarises AA-size nickel–zinc cells with nickel hydroxide electrodes of one or two layers and also includes cells with electrodes of different foam thickness and paste composition. The quantity of zinc anode, nickel cathode and the zinc/nickel hydroxide ratio as well as the nickel hydroxide utilisation is listed in this table. Cells containing two nickel hydroxide layers provide reduced volume for the zinc anode gel, as mentioned previously. Consequently, these cells have a very low zinc/nickel hydroxide ratio of only 1.12–1.19. The corresponding values of cells with single-layered nickel hydroxide electrodes of the same foam type, Retec 80 and 110, range from 2.62 to 3.21. AA-size nickel–zinc cells with two nickel hydroxide layers reached only 54–60% utilisation of active mass, based on the calculation of maximum discharge capacity. On the contrary, cells with single-layered nickel electrodes of this series obtained better nickel hydroxide utilisation of 76–82%.

3.3. Effect of paste composition on cell performance of nickel–zinc cells

The addition of nickel and cobalt powder to nickel hydroxide slurry was studied to investigate the effect of these additives on cell performance and cycle life of cylindrical nickel–zinc cells. Various nickel hydroxide electrodes containing different amount of nickel (0–8.6 wt.%) and cobalt powder (0–8 wt.%) in the slurry were prepared in the single-layered electrode version with the 2.2 mm Inco foam.

Fig. 8 shows the effect of paste composition on cell performance of AA-size nickel–zinc cells after formation cycling at the 10th cycle. The first group of cells with varying cobalt amounts was prepared with 8.6% nickel powder. The second group with different nickel additions was made with 4.3% cobalt. From Fig. 8 it can be concluded that discharge capacity strongly depends on cobalt amount. The cell containing no cobalt additive delivered a very low discharge capacity of 374 mAh. The highest capacity value of this group was yielded with 8% cobalt addition, in particular, discharge capacity was improved by 60% in comparison to cells without cobalt. For the second group containing various nickel additives we found that a nickel content of 2% raised discharge capacity by 15% compared to cells without any nickel powder. Between 2 and 8.6% nickel admixture there was no significant difference in discharge capacity.

In order to further study the influence of nickel and cobalt powder on electronic conductivity of nickel electrode, resistivity measurements of PVA-bonded nickel hydroxide films were performed. It is known that the addition of nickel powder improves electronic conductivity of the active nickel hydroxide mass [29]. Cobalt powder enhances conductivity and increases oxygen overpotential as well, and thus ensures better charge efficiency and active-material utilisation of the nickel electrode [30,31]. The resistivity measurements of the nickel hydroxide film were carried out with the Megohmmeter IM6 from Radiometer, Copenhagen. A small microscopic slide was coated with two strips (1 cm^2) of conductive silver paint, leaving a 1 mm gap in between, in order to be covered with the nickel hydroxide film of various amount of nickel and cobalt powder. The preparation of this film was done as described in Section 2.1. The wet slurry mixture was applied with a paintbrush on the microscopic slide and dried prior to the measurement.

Fig. 9 illustrates the resistivity of PVA-bonded nickel hydroxide film as a function of nickel and cobalt concentration. Both of these groups also contained a constant amount of the other metal powder, as mentioned above. From this diagram it is quite clear that the addition of a small amount of cobalt (2%) caused an extreme decline in resistivity by 78%, meaning that the film became more conductive. An addition of cobalt up to 8% only slightly decreased resistivity. The admixture of 2% nickel to the slurry lowered the resistivity by 53%, compared to film without any nickel.

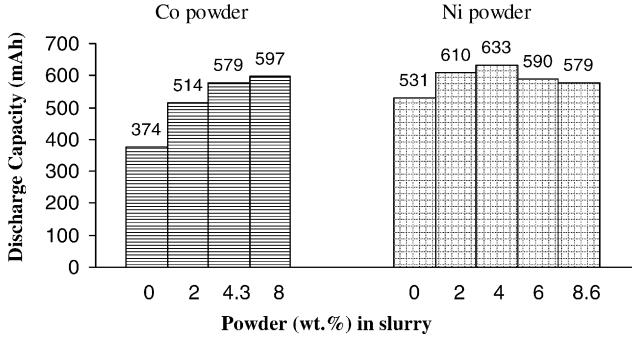

Fig. 8. Effect of paste composition on discharge capacity of AA-size nickel–zinc cells. Discharge: at 3.9 Ω–800 mV (10 cycle). Charge: with 1.90 V constant.

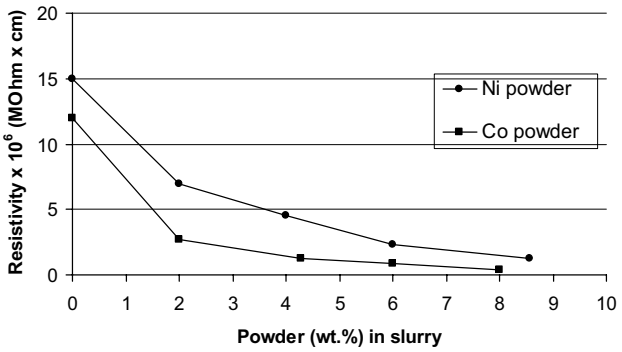

Fig. 9. Resistivity of PVA-bonded nickel hydroxide film as a function of nickel and cobalt powder concentration.

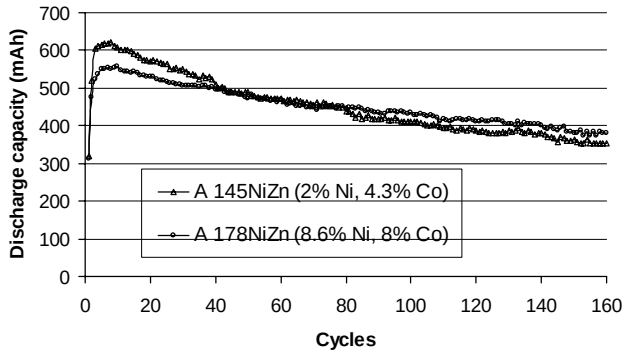

Fig. 10. Discharge capacity of AA-size nickel–zinc cells with different nickel and cobalt additives in slurry vs. cycles. Discharge: at 3.9 Ω–800 mV. Charge: with 1.90 V constant.

Further increasing the nickel addition resulted in a decrease of resistivity, similar but not as great as with cobalt.

For further investigations, AA-size nickel–zinc cells of two opposite cathode slurry compositions were prepared: (a) with high resistivity (2% Ni, 4.3% Co) and (b) with low resistivity (8% Co, 8.6% Ni). In Fig. 10 the discharge performance of these cells can be seen. Cell A 145NiZn, with a minimum of nickel and cobalt, delivered very high discharge capacities up to 40 cycles. This performance was surprising and contrary to what we expected from resistivity measurements. A closer look showed that this behaviour was due to the higher loading of nickel foam, especially with this paste composition, as listed in Table 2. An explanation for this finding is the fact that nickel powder is three times more voluminous than cobalt powder. Therefore, 15% more nickel hydroxide slurry, composed of less nickel, could be pasted into the porous nickel substrate of cell A 145NiZn (Table 2). On the other hand, nickel hydroxide utilisation (57%) and zinc/nickel hydroxide ratio was rather low (1.39) and consequently, discharge capacity decreased more rapidly with increasing cycle life. Cell A 178NiZn, prepared with a maximum of cobalt and nickel additives, delivered lower discharge capacities, up to 40 cycles, in comparison to cell A 145NiZn, as it contained less nickel cathode mass. Regarding cycle life, this cell showed the advantage of minor decrease in discharge capacity after prolonged cycling performance up to 160 cycles, as the zinc/nickel hydroxide ratio was higher (1.78).

4. Conclusions

This work has clearly shown that thicker foam material significantly enhanced discharge capacity. The use of two thinner nickel electrode layers also favoured discharge behaviour at the beginning, however, the capacity declined rapidly during cycle life due to a very low zinc/nickel hydroxide ratio.

From the study that has been carried out with nickel and cobalt additives, we can conclude that small amounts of cobalt and nickel extremely lowered electronic resistivity of nickel hydroxide film. Cycling experiments performed with AA-size nickel–zinc cells have shown that cells prepared of less conductive slurry achieved the highest discharge capacity. This contradictory result can be explained by the fact that an increased foam loading with active material was obtained. The decline in capacity observed during cell cycling was related to a diminished zinc/nickel hydroxide ratio. As the cylindrical cell design is volume limited, the zinc/nickel hydroxide ratio is therefore restricted.

In conclusion, it was demonstrated that the zinc/nickel hydroxide ratio is a key factor for long-term cycling stability of cylindrical nickel–zinc cells. Further studies are required to apply these findings to other cell geometries, e.g. flat cells, in order to avoid limitation of the zinc/nickel hydroxide ratio and to get the entire benefit of improved discharge capacity over the whole cycle life.

References

[1] J.T. Nichols, F.R. McLarnon, E.J. Cairns, Chem. Eng. Commun. 38 (1985) 357–381.
[2] E.G. Gagnon, J. Electrochem. Soc. 133 (1986) 1989–1995.
[3] M. Eisenberg, in: Proceedings of the 34th International Power Sources Symposium, The Electrochemical Society, Pennington, NJ, 25–28 June 1990, pp. 232–234.
[4] E.G. Gagnon, J. Electrochem. Soc. 138 (1991) 3173–3176.
[5] G. Bronoel, A. Millot, N. Tassin, J. Power Sources 34 (1991) 243–255.
[6] R. Jain, T.C. Adler, F.R. McLarnon, E.J. Cairns, J. Appl. Electrochem. 22 (1992) 1039–1048.
[7] T.C. Adler, F.R. McLarnon, E.J. Cairns, J. Electrochem. Soc. 140 (1993) 289–294.
[8] N. Tassin, G. Bronoel, J.F. Fauvarque, A. Millot, in: Proceedings of the 37th Power Sources Conference, Cherry Hill, New Jersey, 17–20 June 1996, pp. 378–381.
[9] W. Taucher, T.C. Adler, F.R. McLarnon, E.J. Cairns, J. Power Sources 58 (1996) 93–97.
[10] A.P. Pavlov, L.K. Grigorieva, S.P. Chizhik, V.K. Stankov, J. Power Sources 62 (1996) 113–116.
[11] D. Coates, E. Ferreira, A. Charkey, J. Power Sources 65 (1997) 109–115.
[12] A. Charkey, D.K. Coates, US Patent 5,863,676 (1999).
[13] Y. Sato, M. Kanda, H. Niki, M. Ueno, K. Murata, T. Shirogami, T. Takamura, J. Power Sources 9 (1983) 147–159.
[14] H.F. Gibbard, R.C. Murray, R.A. Putt, T.W. Valentine, C.J. Menard, US Patent 4,552,821 (1985).
[15] M. Nogami, M. Tadokoro, K. Inoue, N. Furukawa, in: Proceedings of the 40th ISE Meeting, vol. II, Kyoto, Japan, Ext. Abstr., 1989, pp. 1213–1214.
[16] J. Jindra, J. Power Sources 37 (1992) 297–313.
[17] J. Jindra, J. Power Sources 66 (1997) 15–25.
[18] J. Jindra, J. Power Sources 88 (2000) 202–205.
[19] F.R. McLarnon, E.J. Cairns, J. Electrochem. Soc. 138 (1991) 645–664.
[20] J. McBreen, J. Power Sources 51 (1994) 37–44.
[21] D. Coates, A. Charkey, in: D. Linden, T.B. Reddy (Eds.), Handbook of Batteries, McGraw-Hill Inc., New York, 2002, pp. 31.1–31.37.
[22] B. Bugnet, M. Costa, D. Doniat, R. Rouget, in: Proceedings of the 39th Power Sources Conference, Cherry Hill, New Jersey, 12–15 June 2000, pp. 535–538.

[23] B. Bugnet, D. Doniat, R. Rouget, in: Proceedings of the 40th Power Sources Conference, Cherry Hill, New Jersey, 10–13 June 2002, pp. 318–321.
[24] Y.B. Pyun, H. Chang, M.E. Alexeeva, Electrochem. Soc. Proc. 95-14 (1995) 229–240.
[25] W. Taucher-Mautner, K. Kordesch, in: C.F. Holmes, A.R. Landgrebe (Eds.), Proceedings of the Symposium on Batteries for Portable Applications and Electric Vehicles, The Electrochem. Soc., Pennington, NJ, PV 97-18, 1997, pp. 710–716.
[26] W. Taucher-Mautner, K. Kordesch, W. Hartford, PCT Int. Appl., WO 01/18897 A1, 2001.
[27] W. Taucher-Mautner, K. Kordesch, in: G.A. Nazri, E. Takeuchi, R. Koetz, B. Scrosati (Eds.), Proceedings of the Symposium on Batteries and Supercapacitors, The Electrochem. Soc., Pennington, NJ, PV 2001-21, 2003, pp. 695–702.
[28] J. Daniel-Ivad, K. Kordesch, E. Daniel-Ivad, L. Duong, Enhancements to the cycle life of consumer RAM^{TM} Batteries-Marathon RAM^{TM} cells, in: 20th International Seminar and Exhibit on Primary and Secondary Batteries, Ft. Lauderdale, Florida, March 17–20, 2003.
[29] P.J. Kalal, L.M. Timberg, V.A. Ettel, Electrochem. Soc. Proc. 96-14 (1996) 202–211.
[30] A. Yuan, S. Cheng, J. Zhang, C. Cao, J. Power Sources 77 (1999) 178–182.
[31] Z. Chang, Y. Zhao, Y. Ding, J. Power Sources 77 (1999) 69–73.